BIOCHEMISTRY
including biophysical chemistry & molecular biology

Article

pubs.acs.org/biochemistry

Free Cholesterol Determines Reassembled High-Density Lipoprotein Phospholipid Phase Structure and Stability

Matthew Auton,[†,∥] G. Randall Bassett,[‡] Baiba K. Gillard,[§] and Henry J. Pownall*[,§]

[†]Cardiovascular and Thrombosis Research Section, Department of Medicine, Baylor College of Medicine, Houston, Texas 77030, United States

[‡]Department of Molecular Physiology and Biophysics, Baylor College of Medicine, Houston, Texas 77030, United States

[§]Cardiology Department, The Methodist Hospital Research Institute, Houston, Texas 77030, United States

Supporting Information

ABSTRACT: Reassembled high-density lipoproteins (rHDL) of various sizes and compositions containing apo A-I or apo A-II as their sole protein, dimyristoylphosphatidylcholine (DMPC), and various amounts of free cholesterol (FC) have been isolated and analyzed by differential scanning calorimetry (DSC) and by circular dichroism to determine their stability and the temperature dependence of their helical content. Our data show that the multiple rHDL species obtained at each FC mole percent usually do not have the same FC mole percent as the starting mixture and that the size of the multiple species increases in a quantized way with their respective FC mole percent. DSC studies reveal multiple phases or domains that can be classified as virtual DMPC, which contains a small amount of DMPC that slightly reduces the melting temperature (T_m), a boundary phase that is adjacent to the apo A-I or apo A-II that circumscribes the discoidal rHDL, and a mixed FC/DMPC phase that has a T_m that increases with FC mole percent. Only the large rHDL contain virtual DMPC, whereas all contain boundary phase and various amounts of the mixed FC/DMPC phase according to increasing size and FC mole percent. As reported by others, FC stabilizes the rHDL. For rHDL (apo A-II) compared to rHDL (apo A-I), this occurs in spite of the reduced number of helical regions that mediate binding to the DMPC surface. This effect is attributed to the very high lipophilicity of apo A-II and the reduction in the polarity of the interface between DMPC and the aqueous phase with an increasing FC mole percent, an effect that is expected to increase the strength of the hydrophobic associations with the nonpolar face of the amphipathic helices of apo A-II. These data are relevant to the differential effects of FC and apolipoprotein species on intracellular and plasma membrane nascent HDL assembly and subsequent remodeling by plasma proteins.

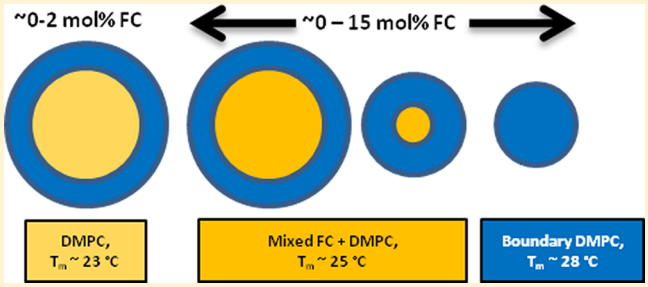

Although cardiovascular disease (CVD)[1] is negatively correlated with plasma high-density lipoprotein-cholesterol (HDL-C), the correlation is not axiomatic because HDL functionality, which is likely related to the properties of HDL, is also important.[2] Thus, the structure and properties of various HDL are relevant to identifying their functional determinants. Apolipoproteins (apos) A-I and A-II, the most abundant HDL-apos (~50 and ~25 μM, respectively, in human plasma), microsolubilize macrophage phospholipids and free cholesterol (FC) via ABCA1 giving nascent HDL.[3,4] Nascent HDL formation in hepatocytes begins by intrahepatic ABCA1-independent apo lipidation in the endoplasmic reticulum followed by ABCA1-dependent lipidation in the Golgi and at the plasma membrane.[5] Half of apo A-I is secreted lipid-free and later transferred to spherical HDL in a lecithin:cholesterol acyltransferase (LCAT)-dependent manner.[6,7] In contrast, apo A-II is fully lipidated and dimeric in the early stages of its intrahepatic processing and occurs on particles without apos A-I and E and only after secretion fuses with apo A-I- and E-containing particles.[7,8] In human plasma, approximately two-thirds of HDL particles contain apo A-I and apo A-II, with the remainder containing apo A-I without apo A-II.[9]

In vitro microsolubilization of dimyristoylphosphatidylcholine (DMPC) multilamellar vesicles (MLV) by apos A-I and A-II produces rHDL, the in vitro analogue of nascent HDL.[10] FC has a profound effect on the kinetics of rHDL formation, which is fastest at ~12.5 mol % cholesterol,[11] the concentration that produces the maximal number of defects for apos to insert between lipid clusters.[11] As with ABCA1-mediated apo A-I lipidation,[3] FC increases the size and number of rHDL species formed by the association of apos A-I and A-II with DMPC.[12,13] rHDL formation is rapid up to 20 mol % FC, above which the rate decreases to nil.[12,13]

Ample data show that apo A-II is more lipophilic than apo A-I. Prolonged centrifugation of HDL sheds apo A-I but not apo A-II;[14] apo A-II displaces apo A-I from HDL,[15] and denaturants or heat disrupts the HDL structure with the release of lipid-free

Received: May 29, 2013
Published: May 30, 2013

   dx.doi.org/10.1021/bi4006732 | *Biochemistry* 2013, 52, 4324−4330

apo A-I but not apo A-II.[16] Many proteins that target HDL, such as LCAT, hepatic lipase, lipid transfer proteins,[17−20] and streptococcal serum opacity factor,[21] disrupt HDL with the concomitant release of lipid-free apo A-I but not apo A-II. Given its greater lipophilicity versus that of apo A-I, we hypothesized that rHDL formed from apo A-II would be more stable than those formed from apo A-I. Using high-sensitivity differential scanning calorimetry (DSC) and the temperature dependence of their circular dichroic spectra, we compared the effects of FC on the stability of rHDL prepared from apos A-I and A-II.

MATERIALS AND METHODS

Chemicals. Glycine and sodium chloride were obtained from Sigma-Aldrich; sodium acetate and EDTA were from ICN Biomedicals, and dibasic sodium phosphate was from Fisher Scientific. All chemicals were of analytical grade or higher purity. All measurements, if not stated differently, were performed using a temperature stable buffer mixture containing 10 mM sodium acetate, 10 mM Na_2PO_4, 10 mM glycine, 150 mM NaCl, and 2 mM EDTA (pH 8).

rHDL Preparation and Labeling. MLV were prepared from ethanolic solutions of DMPC and FC that were reduced to dryness by a stream of nitrogen and over a vacuum for >15 min. The dried lipids were dispersed into Tris-buffered saline (TBS) (10 mM Tris, 100 mM NaCl, 1 mM azide, and 1 mM EDTA) by being vortexed, after which the lipids were subjected to three cycles of warming to 50 °C with vortexing and freezing to −20 °C.

Preparation and Analysis of rHDL Formed from DMPC/Apo-A-I and DMPC/Apo-II Mixtures. Apos A-I and A-II were isolated as described previously.[22,23] Apo concentrations were determined spectrophotometrically.[24] rHDL were prepared by incubating DMPC containing 0−30 mol % FC at the transition temperature of the DMPC, 24 °C, with a DMPC:apo ratio of 10 (w/w). Unbound DMPC was sedimented at 16000*g* for 30 min in an Eppendorf 5415C centrifuge at 4 °C. The rHDL in the supernatant were separated into various rHDL by SEC over tandem columns of Superose HR6 (GE Healthcare) and fractions collected.[12,13] Protein and lipid compositions of the various rHDL species were determined using the Bio-Rad DC protein assay and WAKO phospholipid C and free cholesterol E kits. Molar compositions were calculated using molecular weights of 28016 for apo A-I, 17414 for apo A-II, 760 for PC, 678 for DMPC, and 387 for FC.

Spectroscopy. The protein concentration was quantified spectrophotometrically according to the method of Edelhoch[25] and modified by the method of Pace[26] as $A_{280} - 2A_{333}$ (to correct for light scattering) on a Shimadzu UV2101PC spectrophotometer. Thermal denaturation of rHDL was followed by circular dichroism at 222 nm (Aviv Biomedical model 420C) using a 1 mm quartz cell at a scan rate of 1 °C/min; data were collected every 3 s with an integration time of 0.1 s. Ellipticity θ (millidegrees) was converted to mean residue molar ellipticity {MRME (degrees square centimeters per decimole of residues) = [100θ (millidegrees) × MW (grams per mole)]/[c (milligrams per milliliter) × l (cm) × number of residues]}. We used a Savitsky−Golay numerical derivative to smooth and differentiate the data by a simplified least-squares procedure.[27] The numbers of amino acid residues in apo A-I (28016 Da) and apo A-II (17414 Da) are 243 and 168, respectively.

Calorimetry. The stability of the rHDL lipid component was determined by differential scanning calorimetry (DSC) on a TA Instruments NanoDSC apparatus equipped with a fixed capillary cell design at a pressure of 300 kPa using a scan rate of 1 °C/min. Prior to DSC measurements, buffers and samples were degassed with moderate stirring for 10 min in a vacuum desiccator. The calorimeter was calibrated by performing a cell balance scan and residual scans as described in the manual. The calorimeter was equilibrated overnight with buffer in both the reference and sample cells with repeated thermal scans until a stable baseline was obtained, after which the buffer in the sample cell was replaced with a protein solution during the equilibration step between scans. One measurement per second was recorded between 1 and 95 °C. DSC traces were corrected by subtracting the baseline background buffer scan. Calorimetric power compensation (microjoules per second) was converted to molar heat capacity C_p (kilojoules per mole per degree Kelvin) = power (microjoules per second)/[scan rate (degrees Celcius per minute)/60V (milliliters) × c (micromolar) × 1000]. Excess molar heat capacity was obtained by subtracting an 11th-order polynomial fit to the pre- and post-transition regions of the heat capacity traces using a Mathematica (Wolfram, Inc.) script developed in our laboratory. The transition enthalpies were determined from the total integral of the excess heat capacity.

RESULTS

rHDL Preparation and Isolation. Apos A-I and A-II were incubated with DMPC containing 0, 5, 10, and 15 mol % FC at 24 °C. Excess DMPC was sedimented and the rHDL separated by SEC, a method in which the elution volume (EV) decreases with an increasing particle size (Figure 1). Like that of rHDL (apo A-I), the EV for rHDL (apo A-II) shifts to earlier elution volumes indicative of increased rHDL size as the FC mole percent in the initial incubation mixture increases. The effect of FC on rHDL size appears to be quantized; at some

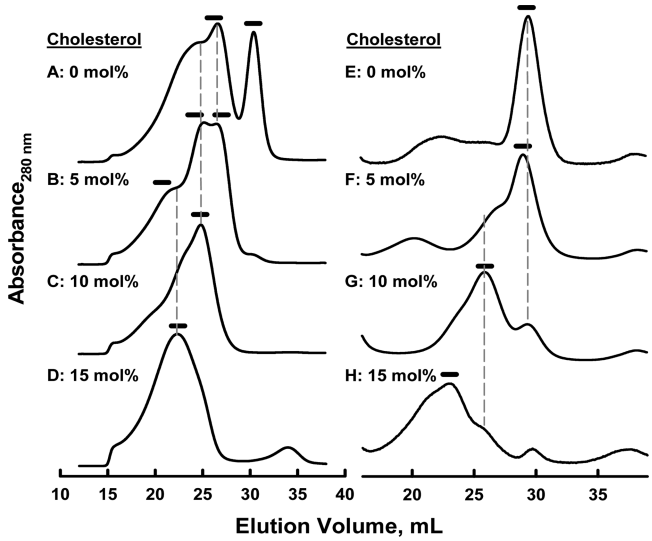

Figure 1. Isolation of rHDL prepared from DMPC and various initial starting FC mole percents as indicated. (A−D) SEC of rHDL (apo A-I) and (E−H) SEC of rHDL (apo A-II). Bars indicate the fractions that were pooled for analysis by DSC and CD. According to SEC principles, the elution volume of the rHDL increases as its particle size decreases.

dx.doi.org/10.1021/bi4006732 | *Biochemistry* 2013, 52, 4324−4330

compositions, a peak in the chromatogram is observed, whereas at higher or lower FC mole percents, only a shoulder may appear. Fractions indicated by the horizontal bars were collected and analyzed by SEC for homogeneity and composition. The collected fractions, though broadly distributed, are homogeneous and almost normally distributed (Figure 2). According to compositional analyses (Figure 3), the

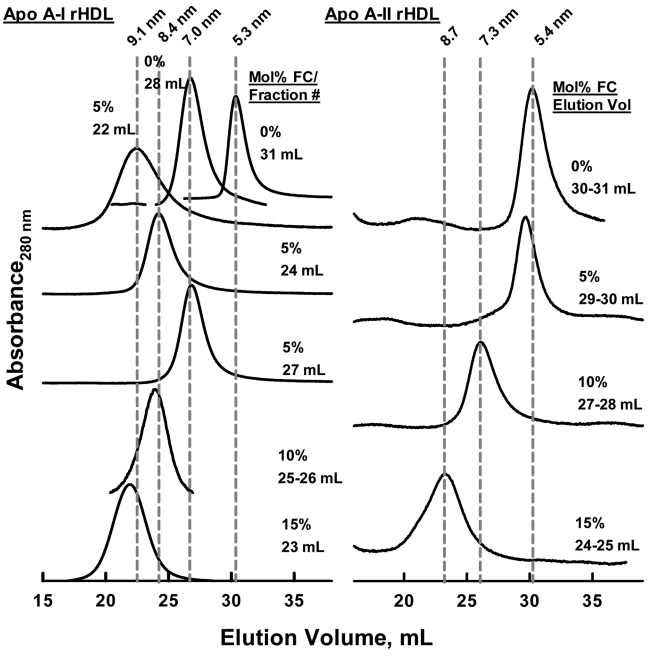

Figure 2. Analytical SEC of the various rHDL. Left panels show the SEC profiles of rHDL (apo A-I); each panel indicates the initial FC mole percent of each rHDL and its respective elution volume. The right panel shows the same data for rHDL (apo A-II). The compositions of each peak are given in Figure 3.

DMPC:apo ratio increased with particle size, with ratios for the smallest and largest rHDL (apo A-I) being 140:1 and 340:1, respectively. The corresponding values for rHDL (apo A-II) were 48:1 and 100:1, respectively. These data also show that at a given initial FC mole percent, multiple semidiscrete rHDL species form that increase in size as their FC mole percent increases. For example, at an initial composition of 5 mol % FC, three species form (Figure 1B). After isolation (Figure 2), the FC contents of the three species (smallest to largest) were 4.5, 5.2, and 5.8 mol %.

Differential Scanning Calorimetry (DSC). DSC of DMPC revealed two endotherms, one at 12.5 °C, a pretransition, and a larger main transition temperature (T_m) at 23.9 °C (Figure 1A of the Supporting Information, 0 mol % FC scan). The pretransition was absent from the DSC of DMPC containing 5 mol % FC, whereas the main transition was broadened, its enthalpy reduced, and its T_m shifted to a slightly lower temperature. This trend continued up to 20 mol % FC where a transition was barely discernible; at 25 mol % FC, there was no detectable transition (Figure 1B–F of the Supporting Information).

The endotherms for all rHDL were broader than those of DMPC with or without FC. Small and/or FC-rich rHDL have symmetrical endotherms. More specifically, the endotherms for the small rHDL (apo A-I) containing 0 and 4.5 mol % FC and for the medium and large rHDL (apo A-I) containing 10 and

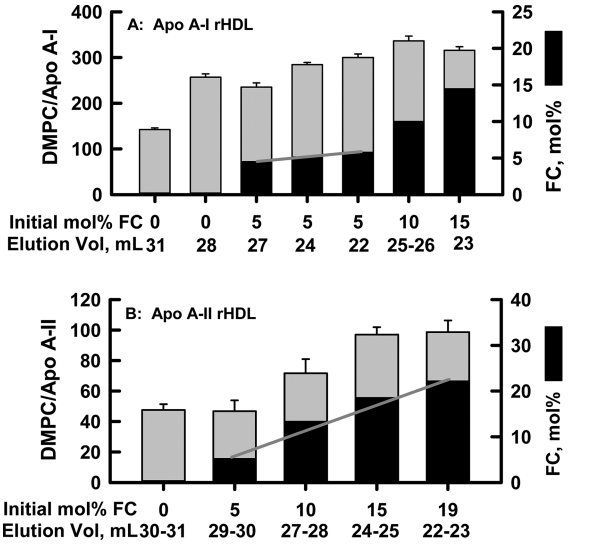

Figure 3. Stoichiometry of rHDL. The analyzed rHDL are those isolated according to Figure 1 and tested for purity in Figure 2. Note that a given initial FC mole percent can yield multiple, differently sized rHDL with FC compositions that are different from those of the starting mixture. For example, at 5 mol % FC, three species of rHDL (apo A-I) are obtained from a starting FC content of 5 mol %. Note also that typically the elution volume decreases (larger size) as the FC mole percent of each rHDL increases.

14.5 mol % FC, respectively, were symmetrical with T_m values of 28.1, 27.3, 27.8, and 28.6 °C, respectively (Figure 4A). In contrast, endotherms for medium and large rHDL (apo A-I) with 0, 5.2, and 5.8 mol % FC were comprised of two components (Figure 4), better discerned in the first derivatives of the endotherm (Figure 2 of the Supporting Information). Large rHDL (apo A-I) with 0 mol % FC exhibited a T_m of 23.0 °C, the same as that of pure DMPC, and 27.0 °C. The endotherms for large and medium size rHDL (apo A-I) containing 5.8 and 5.2 mol % FC exhibited T_m values of 25.0 and 28.0 °C and T_m values of 26.4 and 28.0 °C, respectively. In a second thermal scan of each rHDL, broad endotherms of the first scan were replaced by sharp transitions, similar to that of pure DMPC, superimposed on a broader higher thermal transition whose T_m increased with FC mole percent (Figure 4B).

Similar calorimetric measurements were performed on rHDL (apo A-II). At 0 mol % FC, the T_m appeared as a single broad symmetrical peak, and unlike rHDL (apo A-I), there was no hint of a transition below that of pure DMPC. Like those of rHDL (apo A-I), the T_m increased with an increasing FC mole percent (0, 5.2, 13.4, and 18.5 mol % FC had T_m values of 28.9, 29.3, 29.5, and 31.1 °C, respectively) and the attendant enthalpies of melting decreased to nil with increasing FC content up to 22.2 mol % (Figure 5A and Figure 3 of the Supporting Information). According to the scans and as confirmed by the first derivative of the scans, two weaker thermal transitions appear at 32.4 and 35.0 °C in rHDL (apo A-II) containing 13.4 and 18.5 mol % FC, respectively. The second thermal scan for rHDL (apo A-II) was also distinct from that of rHDL (apo A-I); in the absence of FC, a sharp peak coinciding with that for pure DMPC appeared followed by a higher-temperature shoulder (Figure 5B). With an increasing FC mole percent, the enthalpy of the sharp peak decreased and that of the shoulder increased until at 19 mol % FC, only the

dx.doi.org/10.1021/bi4006732 | Biochemistry 2013, 52, 4324–4330

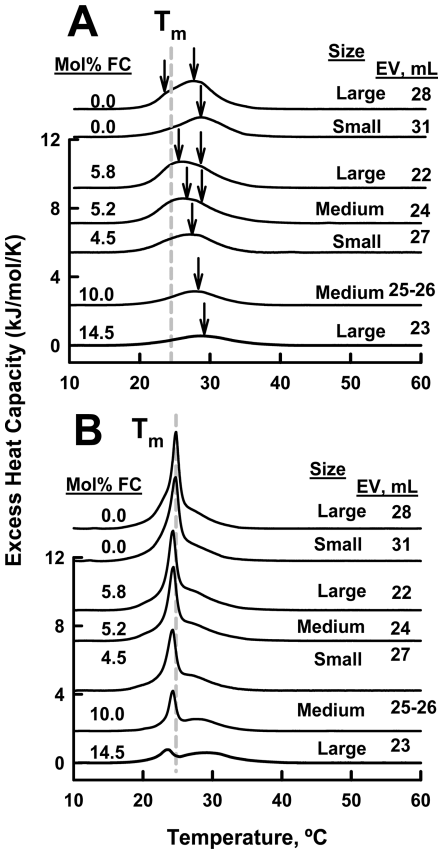

Figure 4. (A) DSC of rHDL (apo A-I). The vertical arrows indicate the melting points, T_m, of each species identified according to the first derivative of the excess heat capacity vs temperature. The vertical dashed gray line is the T_m of DMPC. Note that the larger particles exhibit more than one T_m. The legend associated with each scan denotes the FC mole percent in the rHDL tested and the elution volume (EV) at which it was isolated. (B) Repeat DSC scans of the same rHDL as in panel A. The most prominent features are the replacement of the broad, multicomponent endotherm of panel A with a composite endotherm that includes a T_m for a virtual DMPC phase appearing slightly below that of pure DMPC (vertical dashed gray line). Note the appearance of a second transition defined as the FC/DMPC phase at temperatures higher than that of pure DMPC for the medium (5.2 mol % FC) and large (0 and 5.8 mol % FC) species.

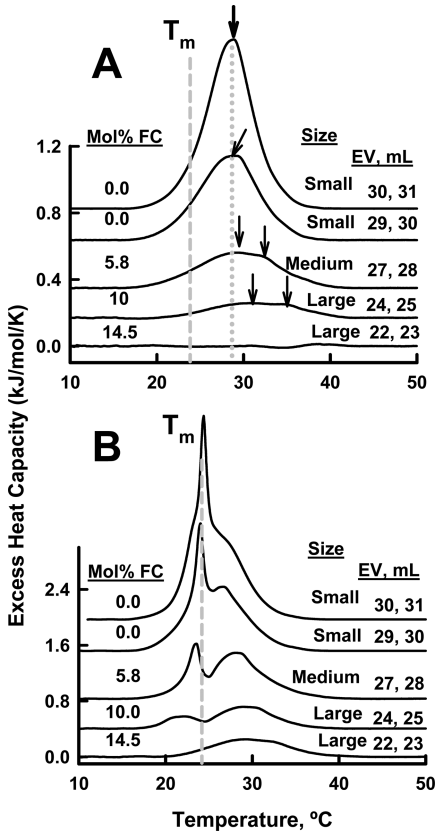

Figure 5. Same as panels A and B of Figure 4 but for rHDL (apo A-II). The vertical dashed gray line is the T_m of DMPC. The dotted gray line is the T_m for 0 mol % FC rHDL. Again, like the second scan of rHDL (apo A-I), the broad first scan endotherm is replaced by two peaks, a sharp one similar to that of DMPC and a broader peak that represents an increasing fraction of the total endotherm as the FC mole percent increases.

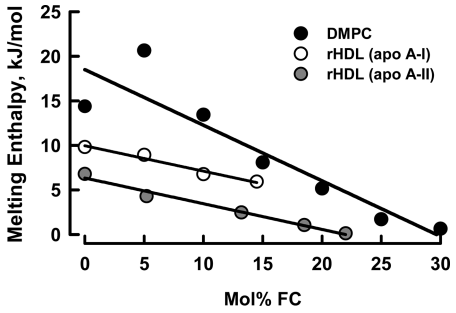

Figure 6. Enthalpy of DMPC melting within rHDL as a function of FC mole percent. Notable features are a lower melting enthalpy for rHDL (apo A-II) than for rHDL (apo A-I). The slopes for the two rHDL are similar but distinct from the much greater slope for DMPC.

broad higher-temperature endotherm was observed. The enthalpies of melting of DMPC and each of the rHDL as a function of FC mole percent are summarized in Figure 6. These data show that the enthalpy of DMPC melting at a given FC mole percent decreases in the following order: DMPC > rHDL (apo A-I) > rHDL (apo A-II). According to the slopes of the curves, the decrease in the enthalpy of melting with added FC for DMPC was greater than that of either rHDL.

Circular Dichroism. Both apo A-I and apo A-II in rHDL have a high α-helical content that can be used to follow temperature-dependent unfolding (Figure 7A,B). The loss of the α-helical content with an increase in temperature reflects the unfolding of the rHDL protein component. The midpoint for the unfolding curve calculated from the second derivative of MRME versus temperature (Figure 4 of the Supporting Information) defines the unfolding transition temperature, which was little changed with respect to FC content for rHDL (apo A-I) but very FC-dependent for rHDL (apo A-II), which exhibited a sharp increase in the T_m as a function of FC mole percent (Figure 7C). As discussed below, previous studies have shown that rHDL formed by the reactions of apo A-I and apo A-II with cholesterol containing DMPC MLV are unstable to heat and dissociate into lipid-free or -poor apos and fusion products above 75 °C.

DISCUSSION

Calorimetric Data. The DSC data are both profound and subtle. In terms of subtlety, our data show that both FC and apos produce a profound broadening of the main DMPC transition. On the subtle side, a more thorough analysis of the

dx.doi.org/10.1021/bi4006732 | Biochemistry 2013, 52, 4324−4330

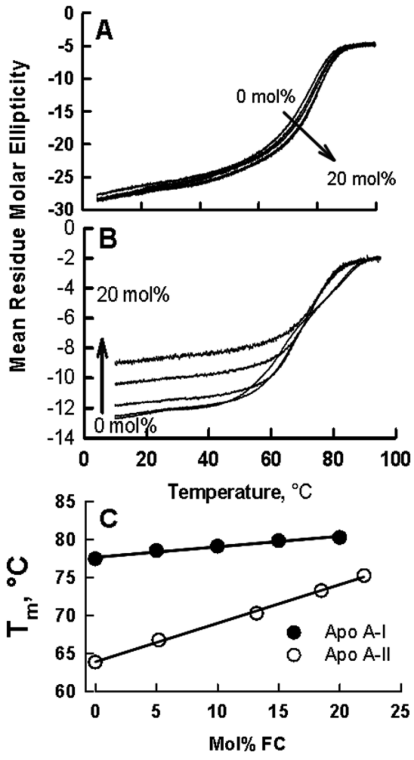

Figure 7. Thermal unfolding of rHDL as assessed by the magnitude of the CD spectrum at 222 nm, which senses α-helical content. Notable features are the similarity of the MRME vs temperature plots for all rHDL (apo A-I) (A) irrespective of FC content. The data for rHDL (apo A-II) are more complicated (B) and show the loss of α-helical content with an increasing FC mole percent and a profound increase in T_m with FC mole percent (see also Figure 4 of the Supporting Information). (C) Differences in stability assessed from the temperature dependence of the T_m from panels A and B vs FC mole percent. Both rHDL are stabilized by FC, i.e., have higher T_m values. rHDL stability increases with added cholesterol faster for rHDL (apo A-II) than for rHDL (apo A-I).

data, in part according to the first derivatives of the DSC data, uncovered evidence of multiple lipid melting transitions that were a function the size of the rHDL, and the FC mole percent contained therein. The rHDL have been studied previously. However, this study differs from those previously reported in a number of ways. First, our rHDL were prepared by incubation of a great molar excess of DMPC with the apos so that multiple rHDL with different sizes and FC mole percents were formed at each initial FC mole percent. Second, noting that the FC mole percent in the rHDL does not always reflect that of the starting mixture, we determined the FC mole percent in each of the isolated complexes, which were relatively homogeneous according to SEC. Lastly, we determined the enthalpies of DMPC melting within the various rHDL complexes. These experimental differences allowed us to refine the current model of FC-containing discoidal rHDL.

Whereas DMPC dispersed in buffer occurs as MLV, according to current models, rHDL has a discoidal structure even in the presence of up to ~20 mol % FC.[12] The effects of FC on the endotherms of pure DMPC are similar to those reported by others who observed that at 14 mol % FC the endotherms can be decomposed into narrow and broad peaks with the T_m of the former, a "virtual DMPC" phase, being equal to or slightly lower than that of pure DMPC and containing a trace of FC and the latter, a more FC-rich phase, having a higher T_m that increases with FC mole percent.[28] Others, like us, have observed that the DMPC (0 mol % FC) T_m for rHDL (apo A-I) is lower than that of pure DMPC and that the thermal unfolding of apo A-II within rHDL occurs at a temperature lower than that of apo A-I.[29,30] Moreover, increasing the FC content increases particle size[12,13,31] and the negative charge on apo A-I while reducing the free energy of apo A-I α-helix stabilization.[31]

rHDL (apo A-I) and rHDL (apo A-II) share many similarities. In the absence of FC, they both occur as quasi-discrete particles, and as the FC mole percent increases, additional larger particles are formed. Small, medium, and large rHDL (apo A-I) are nearly the same size as the respective rHDL (apo A-II). The particle sizes do not increase continuously with an increasing FC mole percent but rather appear to be quantized so that they occur as discrete species. This has been attributed to an increase in domain size with the addition of FC, so that additional apos are needed to fully circumscribe the domain[12,13] and form a disk.

The calorimetric data collected on rHDL support a model with DMPC in three different phases (Figure 8). These are (a)

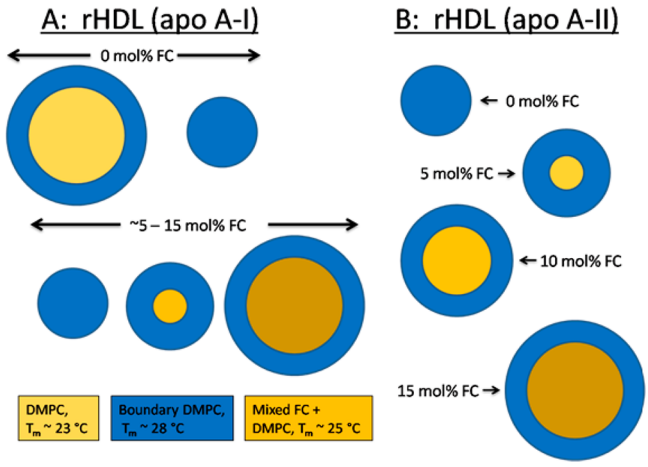

Figure 8. Model of rHDL phases based on DSC data. This model shows that the number of phases within rHDL increases with the FC mole percent and particle size. The increasing shading intensity represents increased FC content within the FC/DMPC phase. The smallest rHDL contain only a boundary DMPC phase.

virtual DMPC, (b) boundary DMPC, i.e., DMPC with a T_m of ~28 °C that is in direct or near-direct contact with the apolipoprotein from which FC is largely excluded, and (c) a mixed FC/DMPC phase that has a transition temperature that increases from ~25 to ~35 °C with an increasing FC mole percent. Both boundary and mixed FC/DMPC phases have a peak T_m 3−5 °C above that of the virtual DMPC. According to this model (Figure 8), the large rHDL (apo A-I) with 0 mol % FC contains a virtual DMPC phase with a T_m of 23.0 °C and a boundary phase with a T_m of 27.0 °C. Large (5.8 mol % FC) and medium (5.2 mol % FC) rHDL (apo A-I) contain mixed FC/DMPC phases with T_m values of 25.0 and 26.4 °C and a boundary phase with a T_m of 28.0 °C. The small (4.5 mol % FC), medium (10.0 mol % FC), and large (14.5 mol % FC) rHDL (apo A-I) have both boundary and mixed FC/DMPC phases melting at 27.3, 27.8, and 28.6 °C. As the size and FC content of rHDL (apo A-I) increase, one would expect the level of the boundary lipid to increase linearly with size and the level of the mixed FC/DMPC phase to increase as the square of the

dx.doi.org/10.1021/bi4006732 | Biochemistry 2013, 52, 4324−4330

size so that the T_m of the largest, most FC-rich rHDL (apo A-I) would be dominated by the melting of the mixed FC/DMPC phase. This was the large rHDL (apo A-I) containing 14.5 mol % FC, which has a T_m of 28.6 °C. Thus, it is likely that the T_m of the mixed FC/DMPC phase is higher than that of boundary DMPC, particularly at a high FC mole percent. In the context of our three-phase model, the calorimetric data for rHDL (apo A-II) were distinct from those of apo A-I. Unlike rHDL (apo A-I), rHDL (apo A-II) exhibits no T_m for virtual DMPC. However, like the endotherms for rHDL (apo A-I), the T_m for rHDL (apo A-II) also increases with an increasing FC mole percent, thereby corroborating the hypothesis that the T_m for the FC/DMPC phase increases with an increasing FC mole percent.

The DSC results of both rHDL (apo A-I) and rHDL (apo A-II) after the first heating and cooling cycle were different (Figures 4B and 5B) from the first scans, indicating that the rHDL structure has been disrupted in a way that was not reversed over the time scale of the cooling cycle.

Circular Dichroism Data. Like others,[29] we observed that the protein unfolding transition is lower for rHDL (apo A-II) than for rHDL (apo A-I) and that the size and unfolding transition temperature increase with an increasing FC mole percent in rHDL (apo A-II). In addition, we found a linear increase in the protein T_m with FC mole percent for both rHDL, with the rate being greater for rHDL (apo A-II) even though its T_m in the absence of FC is lower (Figure 7).

According to their respective MRME at 0 mol % FC, the α-helicity of rHDL (apo A-I) at 10 °C is greater than that of rHDL (apo A-II). Moreover, the α-helicity of rHDL (apo A-I) is independent of FC content at all temperatures studied, whereas the α-helicity of rHDL (apo A-II) decreases with an increasing FC mole percent. The T_m for rHDL (apo A-I) and rHDL (apo A-II) increases with FC mole percent with slopes of 1.4 ± 0.13 and 5.1 ± 0.14 °C/mol %, respectively (Figure 7C). Gursky et al.[16] showed that spherical HDL resides in a kinetic trap from which it escapes by thermal and chaotropic perturbation during which some but not all apo A-I are transferred to the aqueous phase. Moreover, thermal perturbation of rHDL (apo A-I) and rHDL (apo A-II) also liberates lipid-free apos.[32] Thus, the changes observed in the temperature dependence of the CD melting curves are a superposition of apo A-I and apo A-II desorption and likely changes in apo A-I and apo A-II that remain lipid-bound. During heating, the total α-helical content of the system is reduced because the desorbed apos have less α-helicity than lipidated apos.

A major effect of FC is increased rHDL stability, especially for rHDL (apo A-II). This may be due to the well-documented effect of FC on the quality of the water−DMPC interface. FC modulates the depth of penetration of water into lipid bilayers[33] and decreases their interfacial polarity[34] and level of hydration.[35] Association of the apos with phospholipids is mediated by the hydrophobic effect whereby the nonpolar face of the amphipathic helix inserts into and associates with the phospholipid interface. Reducing the polarity and increasing the hydrophobicity of the interfacial region would be expected to amplify the hydrophobic effect and stabilize rHDL (apo A-II). The greater stabilizing effect of FC on rHDL (apo A-II) may be due to the greater enhancement of the already stronger hydrophobic association of apo A-II, the more lipophilic of the two apos.

Our studies are relevant to the mechanisms by which HDL are assembled. Early intracellular forms of HDL include those that contain apo A-II but no apo A-I or apo E.[7] Thus, the rHDL (apo A-II) is a rational biophysical model of a nascent HDL. However, to date the lipid composition of hepatocyte nascent HDL (apo A-II) is not known, so firm conclusions cannot be formulated. The surface of mature forms of human HDL is ~25 mol % FC and, according to our data, nearly saturated in terms of the amount of FC that can be spontaneously incorporated into a phospholipid. Although they are based on a non-physiological PC, our data suggest that FC affects the conformation of apo A-II, which would have decreasing helical content as the FC content is increased. In addition, the presence of FC in HDL could increase the lipophilicity of apo A-II for HDL, thereby stabilizing the LpA-II structure. Thus, it would be interesting to determine whether increasing or decreasing the HDL FC content effects HDL stability and apo A-II conformation and to determine whether macrophage-derived HDL is more or less stable than mature forms of HDL. Future studies will reveal the effects of adding or removing FC from HDL on the conformation and stability of apo A-II versus those of apo A-I.

■ ASSOCIATED CONTENT

Supporting Information

DSC of DMPC MLV as a function of FC mole percent (Figure 1), identification of DMPC T_m values in rHDL (apo A-I) of different sizes and with different FC contents (Figure 2), identification of DMPC T_m values in rHDL (apo A-II) of different sizes and with different FC contents (Figure 3), and identification of the midpoint of the melting curve for rHDL (apo A-I) and rHDL (apo A-II) (Figure 4). This material is available free of charge via the Internet at http://pubs.acs.org.

■ AUTHOR INFORMATION

Corresponding Author

*Address: 6670 Bertner Ave., Houston, TX 77030. E-mail: hjpownall@tmhs.org. Phone: (713) 441-7048.

Present Address

‖M.A.: Division of Hematology, Department of Internal Medicine and Department of Biochemistry and Molecular Biology, Mayo Clinic, Rochester, MN 55905.

Funding

Supported by grants-in-aid from the National Institutes of Health (HL-30914 and HL-56865 to H.J.P. and HL109109 to M.A.).

Notes

The authors declare no competing financial interest.

■ ABBREVIATIONS

ABCA1, ATP-binding cassette transporter A1; apo, apolipoprotein; C, cholesterol; CD, circular dichroism; CVD, cardiovascular disease; DMPC, dimyristoylphosphatidylcholine; DSC, differential scanning calorimetry; EV, elution volume; FC, free cholesterol; HDL, high-density lipoprotein(s); LCAT, lecithin:cholesterol acyltransferase; MLV, multilamellar vesicles; PC, phosphatidylcholine; SEC, size exclusion chromatography; T_m, melting temperature.

■ REFERENCES

(1) Roger, V. L., Go, A. S., Lloyd-Jones, D. M., Benjamin, E. J., Berry, J. D., Borden, W. B., Bravata, D. M., Dai, S., Ford, E. S., Fox, C. S.,

Fullerton, H. J., Gillespie, C., Hailpern, S. M., Heit, J. A., Howard, V. J., Kissela, B. M., Kittner, S. J., Lackland, D. T., Lichtman, J. H., Lisabeth, L. D., Makuc, D. M., Marcus, G. M., Marelli, A., Matchar, D. B., Moy, C. S., Mozaffarian, D., Mussolino, M. E., Nichol, G., Paynter, N. P., Soliman, E. Z., Sorlie, P. D., Sotoodehnia, N., Turan, T. N., Virani, S. S., Wong, N. D., Woo, D., and Turner, M. B. (2012) Executive summary: Heart disease and stroke statistics—2012 update: A report from the American Heart Association. *Circulation 125*, 188−197.

(2) Khera, A. V., Cuchel, M., de la Llera-Moya, M., Rodrigues, A., Burke, M. F., Jafri, K., French, B. C., Phillips, J. A., Mucksavage, M. L., Wilensky, R. L., Mohler, E. R., Rothblat, G. H., and Rader, D. J. (2011) Cholesterol efflux capacity, high-density lipoprotein function, and atherosclerosis. *N. Engl. J. Med. 364*, 127−135.

(3) Liu, L., Bortnick, A. E., Nickel, M., Dhanasekaran, P., Subbaiah, P. V., Lund-Katz, S., Rothblat, G. H., and Phillips, M. C. (2003) Effects of apolipoprotein A-I on ATP-binding cassette transporter A1-mediated efflux of macrophage phospholipid and cholesterol: Formation of nascent high density lipoprotein particles. *J. Biol. Chem. 278*, 42976−42984.

(4) Oram, J. F., and Yokoyama, S. (1996) Apolipoprotein-mediated removal of cellular cholesterol and phospholipids. *J. Lipid Res. 37*, 2473−2491.

(5) Maric, J., Kiss, R. S., Franklin, V., and Marcel, Y. L. (2005) Intracellular lipidation of newly synthesized apolipoprotein A-I in primary murine hepatocytes. *J. Biol. Chem. 280*, 39942−39949.

(6) Chisholm, J. W., Burleson, E. R., Shelness, G. S., and Parks, J. S. (2002) ApoA-I secretion from HepG2 cells: Evidence for the secretion of both lipid-poor apoA-I and intracellularly assembled nascent HDL. *J. Lipid Res. 43*, 36−44.

(7) Gillard, B. K., Lin, H. Y., Massey, J. B., and Pownall, H. J. (2009) Apolipoproteins A-I, A-II and E are independently distributed among intracellular and newly secreted HDL of human hepatoma cells. *Biochim. Biophys. Acta 1791*, 1125−1132.

(8) Clay, M. A., Pyle, D. H., Rye, K. A., and Barter, P. J. (2000) Formation of spherical, reconstituted high density lipoproteins containing both apolipoproteins A-I and A-II is mediated by lecithin:cholesterol acyltransferase. *J. Biol. Chem. 275*, 9019−9025.

(9) Cheung, M. C., and Albers, J. J. (1984) Characterization of lipoprotein particles isolated by immunoaffinity chromatography. Particles containing A-I and A-II and particles containing A-I but no A-II. *J. Biol. Chem. 259*, 12201−12209.

(10) Vedhachalam, C., Duong, P. T., Nickel, M., Nguyen, D., Dhanasekaran, P., Saito, H., Rothblat, G. H., Lund-Katz, S., and Phillips, M. C. (2007) Mechanism of ATP-binding cassette transporter A1-mediated cellular lipid efflux to apolipoprotein A-I and formation of high density lipoprotein particles. *J. Biol. Chem. 282*, 25123−25130.

(11) Pownall, H. J., Massey, J. B., Kusserow, S. K., and Gotto, A. M., Jr. (1979) Kinetics of lipid−protein interactions: Effect of cholesterol on the association of human plasma high-density apolipoprotein A-I with L-α-dimyristoylphosphatidylcholine. *Biochemistry 18*, 574−579.

(12) Massey, J. B., and Pownall, H. J. (2008) Cholesterol is a determinant of the structures of discoidal high density lipoproteins formed by the solubilization of phospholipid membranes by apolipoprotein A-I. *Biochim. Biophys. Acta 1781*, 245−253.

(13) Bassett, G. R., Gillard, B. K., and Pownall, H. J. (2012) Cholesterol Determines and Limits rHDL Formation from Human Plasma Apolipoprotein A-II and Phospholipid Membranes. *Biochemistry 51*, 8627−8635.

(14) Kunitake, S. T., and Kane, J. P. (1982) Factors affecting the integrity of high density lipoproteins in the ultracentrifuge. *J. Lipid Res. 23*, 936−940.

(15) Edelstein, C., Halari, M., and Scanu, A. M. (1982) On the mechanism of the displacement of apolipoprotein A-I by apolipoprotein A-II from the high density lipoprotein surface. Effect of concentration and molecular forms of apolipoprotein A-II. *J. Biol. Chem. 257*, 7189−7195.

(16) Mehta, R., Gantz, D. L., and Gursky, O. (2003) Human plasma high-density lipoproteins are stabilized by kinetic factors. *J. Mol. Biol. 328*, 183−192.

(17) Silver, E. T., Scraba, D. G., and Ryan, R. O. (1990) Lipid transfer particle-induced transformation of human high density lipoprotein into apolipoprotein A-I-deficient low density particles. *J. Biol. Chem. 265*, 22487−22492.

(18) Liang, H. Q., Rye, K. A., and Barter, P. J. (1996) Remodelling of reconstituted high density lipoproteins by lecithin:cholesterol acyltransferase. *J. Lipid Res. 37*, 1962−1970.

(19) Settasatian, N., Duong, M., Curtiss, L. K., Ehnholm, C., Jauhiainen, M., Huuskonen, J., and Rye, K. A. (2001) The mechanism of the remodeling of high density lipoproteins by phospholipid transfer protein. *J. Biol. Chem. 276*, 26898−26905.

(20) Rao, R., Albers, J. J., Wolfbauer, G., and Pownall, H. J. (1997) Molecular and macromolecular specificity of human plasma phospholipid transfer protein. *Biochemistry 36*, 3645−3653.

(21) Gillard, B. K., Courtney, H. S., Massey, J. B., and Pownall, H. J. (2007) Serum opacity factor unmasks human plasma high-density lipoprotein instability via selective delipidation and apolipoprotein A-I desorption. *Biochemistry 46*, 12968−12978.

(22) Brewer, H. B., Jr., Ronan, R., Meng, M., and Bishop, C. (1986) Isolation and characterization of apolipoproteins A-I, A-II, and A-IV. *Methods Enzymol. 128*, 223−246.

(23) Pownall, H. J., Massey, J. B., Kusserow, S. K., and Gotto, A. M., Jr. (1978) Kinetics of lipid−protein interactions: Interaction of apolipoprotein A-I from human plasma high density lipoproteins with phosphatidylcholines. *Biochemistry 17*, 1183−1188.

(24) Pownall, H. J., and Massey, J. B. (1986) Spectroscopic studies of lipoproteins. *Methods Enzymol. 128*, 515−518.

(25) Edelhoch, H. (1967) Spectroscopic determination of tryptophan and tyrosine in proteins. *Biochemistry 6*, 1948−1954.

(26) Pace, C. N., Vajdos, F., Fee, L., Grimsley, G., and Gray, T. (1995) How to measure and predict the molar absorption coefficient of a protein. *Protein Sci. 4*, 2411−2423.

(27) Savitzky, A., and Golay, M. J. E. (1964) Smoothing and Differentiation of Data by Simplified Least Squares Procedures. *Anal. Chem. 36*, 1627−1639.

(28) Mabrey, S., Mateo, P. L., and Sturtevant, J. M. (1978) High-sensitivity scanning calorimetric study of mixtures of cholesterol with dimyristoyl- and dipalmitoylphosphatidylcholines. *Biochemistry 17*, 2464−2468.

(29) Jayaraman, S., Gantz, D. L., and Gursky, O. (2005) Kinetic stabilization and fusion of apolipoprotein A-2:DMPC disks: Comparison with apoA-1 and apoC-1. *Biophys. J. 88*, 2907−2918.

(30) Jayaraman, S., Benjwal, S., Gantz, D. L., and Gursky, O. (2010) Effects of cholesterol on thermal stability of discoidal high density lipoproteins. *J. Lipid Res. 51*, 324−333.

(31) Sparks, D. L., Davidson, W. S., Lund-Katz, S., and Phillips, M. C. (1993) Effect of cholesterol on the charge and structure of apolipoprotein A-I in recombinant high density lipoprotein particles. *J. Biol. Chem. 268*, 23250−23257.

(32) Reijngoud, D. J., and Phillips, M. C. (1982) Mechanism of dissociation of human apolipoprotein A-I from complexes with dimyristoylphosphatidylcholine as studied by guanidine hydrochloride denaturation. *Biochemistry 21*, 2969−2976.

(33) Simon, S. A., McIntosh, T. J., and Latorre, R. (1982) Influence of cholesterol on water penetration into bilayers. *Science 216*, 65−67.

(34) Kao, Y. J., Soutar, A. K., Hong, K. Y., Pownall, H. J., and Smith, L. C. (1978) N-(2-Naphthyl)-23,24-dinor-5-cholen-22-amin-3β-ol, a fluorescent cholesterol analogue. *Biochemistry 17*, 2689−2696.

(35) Massey, J. B., She, H. S., and Pownall, H. J. (1985) Interfacial properties of model membranes and plasma lipoproteins containing ether lipids. *Biochemistry 24*, 6973−6978.